

HETEROCYCLES, Vol. 100, No. 4, 2020, pp. 633 - 644. © 2020 The Japan Institute of Heterocyclic Chemistry  
Received, 17th January, 2020, Accepted, 26th February, 2020, Published online, 2nd March, 2020  
DOI: DOI: 10.3987/COM-20-14213

## SYNTHESIS AND FLUORESCENCE OF 9-BENZYL-9H-CARBAZOLE DERIVATIVES AND ITS APPLICATION FOR RECOGNITION OF RARE EARTH CATIONS

Yu-Ying Du, Li-Min Han,\* Liang-Wu Guo, Zhi-Chao She, Jing Cui, Li Lv, and Ruo-Xuan Gao

Department of Chemical Engineering, Inner Mongolia University of Technology, Huhhot 010051, PR China. E-mail: hhhtdy@163.com, hanlimin@imut.edu.cn

**Abstract** – The synthesis and photophysical properties of 9-benzyl-9H-carbazole derivatives have been investigated. A novel ethyl 9-benzyl-1-methyl-9H-carbazole-2-carboxylate (**Bncz 1**) fluorescent chemosensor has been developed to recognize Ce(III) through a significant increase in fluorescence intensity in ethanol, whereas there is minimal difference on the introduction of the other rare earth metal cations (Yb<sup>3+</sup>, Sm<sup>3+</sup>, Gd<sup>3+</sup>, Er<sup>3+</sup>, Pr<sup>3+</sup>, Eu<sup>3+</sup>, Tb<sup>3+</sup>, Tm<sup>3+</sup>, Dy<sup>3+</sup>, Ho<sup>3+</sup>, Nd<sup>3+</sup>, Lu<sup>3+</sup>, Y<sup>3+</sup>, Sc<sup>3+</sup>, La<sup>3+</sup>). A moderate association constant of  $K = 2.419 \times 10^5 \text{ L} \cdot \text{mol}^{-1}$  has been determined by fluorescence titration, and the corresponding Job's plot analysis indicated 1:1 binding for metal complex formation. The linear increase in fluorescence intensity in response to different concentrations of Ce<sup>3+</sup> gives a low limit of detection of  $7.269 \times 10^{-6} \text{ M}$ . 9-Benzyl-9H-carbazole derivative probe has a **great potential** for the detection of rare earth metal cations.

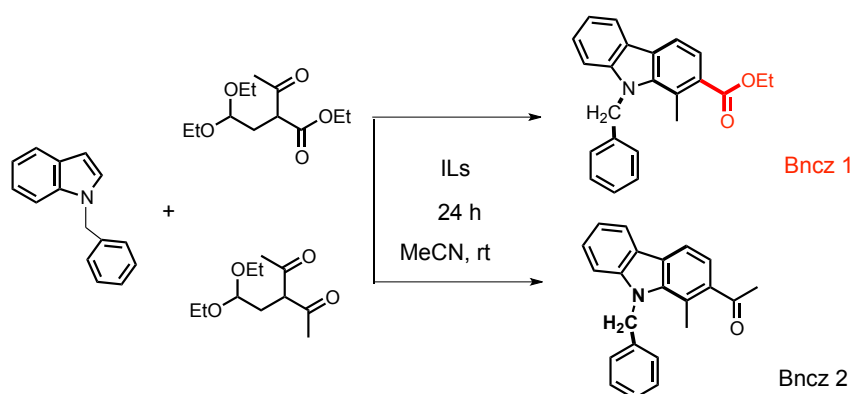
Rare earths are a group of 17 minerals elements including lanthanides, scandium and yttrium. Being physically and chemically similar to one another that collectively, the rare earths could be considered as one element. Moreover, their similar ionic radii and outer electronic structures would make the distinction and separation to be difficulty. However, the rare earth elements have the enormous impact on modern technology and our daily lives, such as photoluminescent, catalysis, metallurgy, energy materials, biology, glass, etc.<sup>1</sup>

Cerium, atomic number 58, is the most abundant rare earth element with the exception of the highly-unstable promethium, which is found in relatively high concentrations in the earth's crust.<sup>2,3</sup> Cerium element is widespreadly used to mirrors, the windshield, cracking catalysts of

the gasoline or diesel fuel, lenses and the three-way catalytic converter in the exhaust products.<sup>4</sup> In view of the limited reserves, low concentration and high value of the rare earth metals, detection and recycling cerium(III) is expected to become more vital to many modern technologies and environment.

The structural core of carbazole is omnipresent in natural products and biologically active compounds.<sup>5-8</sup> Because of their extensive  $\pi$ -conjugation and structural rigidity, carbazole derivatives are widely used in the synthesis of the chromophores and organic photoelectronic materials.<sup>9-12</sup> The study of fluorescent carbazole derivatives for the purpose of sensing has been studied over the past decade.<sup>13-15</sup> However, there are no reports of carbazole derivatives probes for the recognition of rare earth cation so far. Therefore, the design and synthesis of fluorescent carbazole derivatives probes, depending on the properties of rare earth elements, for detection of rare earth element are of great importance.

In this work, we designed and synthesized a carbazole derivative, 9-benzyl-9*H*-carbazole chemosensor, using substituted 1,4-dicarbonyl compounds and indole under mild condition (**Scheme 1**). The chemosensor was applied for recognition towards  $\text{Ce}^{3+}$  cations successfully in ethanol.



**Scheme 1.** Synthesis of probe **Bncz 1** or **Bncz 2**

### Synthesis and characterization

**Bncz 1** and **Bncz 2** were prepared according to the methods developed in our laboratory.<sup>3</sup> As shown in **Scheme 1**, 9-benzyl-9*H*-carbazole derivatives were synthesized by 3-(2,2-diethoxyethyl)-1,3-dicarbonyl compounds and 1-benzyl-1*H*-indole using [Bpy]HSO<sub>4</sub> acid ionic liquid as catalyst under mild condition.

**Bncz 1** and **Bncz 2** were characterized by FT-IR, <sup>1</sup>H NMR and <sup>13</sup>C NMR.

### UV-visible absorption studies

We first examined the differences of the absorption and fluorescent spectra of **Bncz 1** using ethanol solution (10  $\mu\text{M}$ ). As shown in **Figure 1**, the absorption and fluorescence spectra both showed significant differences. The UV-vis spectra of **Bncz 1** showed the absorption of 214, 234, 297, 342 nm, respectively. This charge transfer is due to the intramolecular  $\pi$ - $\pi^*$  or  $n$ - $\pi^*$  transition. No absorption peak of **Bncz 1** was observed in the visible wavelength region. Then the UV-vis absorption spectra of **Bncz 1** with 1.0

equiv. of rare earth metal ions ( $\text{Yb}^{3+}$ ,  $\text{Sm}^{3+}$ ,  $\text{Gd}^{3+}$ ,  $\text{Er}^{3+}$ ,  $\text{Pr}^{3+}$ ,  $\text{Eu}^{3+}$ ,  $\text{Tb}^{3+}$ ,  $\text{Tm}^{3+}$ ,  $\text{Dy}^{3+}$ ,  $\text{Ho}^{3+}$ ,  $\text{Nd}^{3+}$ ,  $\text{Lu}^{3+}$ ,  $\text{Y}^{3+}$ ,  $\text{Sc}^{3+}$ ,  $\text{La}^{3+}$ ,  $\text{Ce}^{3+}$ ) were also compared in the presence of  $\text{NO}_3^-$  anion. The changes in the UV–vis absorption spectra of the free **Bncz 1** upon addition of the various rare earth metal cations are collected in **Figure 1a**. Interestingly, on addition of  $\text{Ce}^{3+}$  cation, the UV–vis absorption spectrum of **Bncz 1** greatly changed, and the obtained spectrum is different to that of **Bncz 1** and other rare earth metal ions. Subsequently, we gradual increase in added  $\text{Ce}^{3+}$  amount (1.0 to 7.0 equiv.) to **Bncz 1** solution, the intensity (at 224 nm) of the solution enhanced gradually and reached a plateau when 7.0 equiv. of  $\text{Ce}^{3+}$  was used and the absorption band transition from 224 to 228 nm (**Figure 1b**).

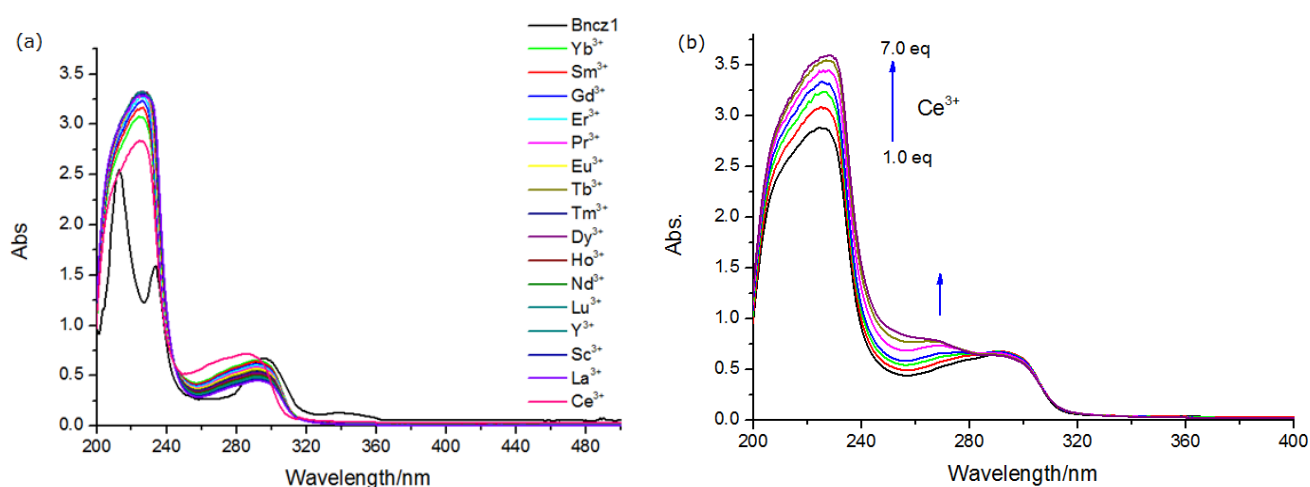


**Figure 1.** (a) UV–vis absorption spectra of **Bncz 1** observed upon addition of 1.0 equiv. of various rare earth metal ions in EtOH (10  $\mu\text{M}$ ); (b) UV–vis absorption spectra of **Bncz 1** observed on addition of 1.0–7.0 equiv. of  $\text{Ce}(\text{NO}_3)_3$  in EtOH (10  $\mu\text{M}$ ).

Then the influence of  $\text{Ce}(\text{NO}_3)_3$  concentration on fluorescence intensity was studied. The changes in the fluorescence intensity at  $\lambda_{\text{em}} = 346$  nm of the free **Bncz 1** and upon addition of the various rare earth metal cations, are collected in **Figure 2a**. The fluorescence intensity of free **Bncz 1** is very low, and minimal differences are observed after the addition of 1.0 equiv. of rare earth metal cations ( $\text{Yb}^{3+}$ ,  $\text{Sm}^{3+}$ ,  $\text{Gd}^{3+}$ ,  $\text{Er}^{3+}$ ,  $\text{Pr}^{3+}$ ,  $\text{Eu}^{3+}$ ,  $\text{Tb}^{3+}$ ,  $\text{Tm}^{3+}$ ,  $\text{Dy}^{3+}$ ,  $\text{Ho}^{3+}$ ,  $\text{Nd}^{3+}$ ,  $\text{Lu}^{3+}$ ,  $\text{Y}^{3+}$ ,  $\text{Sc}^{3+}$ ,  $\text{La}^{3+}$ ), except for  $\text{Ce}^{3+}$  cation. On addition of  $\text{Ce}^{3+}$  cation, a significantly enhanced emission was observed, and the emission pattern is different to that of **Bncz 1** (**Figure 2b**). Fluorescence intensity of the system was increased by increasing the concentration of  $\text{Ce}^{3+}$  solution. Compared to the other rare earth metal cations, as shown in **Figure 2a** and **2b**, it may be implying  $\text{Ce}^{3+}$  cation induced significant increases in the fluorescence intensity of **Bncz 1**,<sup>16</sup> which could be the result from the  $\text{Ce}^{3+}$ –promoted transformation of photo-induced electron-transfer between **Bncz 1** and  $\text{Ce}^{3+}$  cation. This might be explained on the basis of  $\text{Ce}^{3+}$  size and outer electronic structure, which has the larger ionic radius than the other rare earth metal cations, that apparently leads to

geometric and electronic matching with the ligand **Bncz 1** (Scheme 2).<sup>17</sup> On the other hand, cerium has partially filled 4f orbitals shielded by fully occupied 5s and 5p orbitals, and only one electron in its 4f orbital, existing f-f transitions,<sup>18</sup> which could lead to geometric and electronic more suitable for coordination.<sup>19</sup> Therefore, the recognition of  $\text{Ce}^{3+}$  cations could be proceeded.

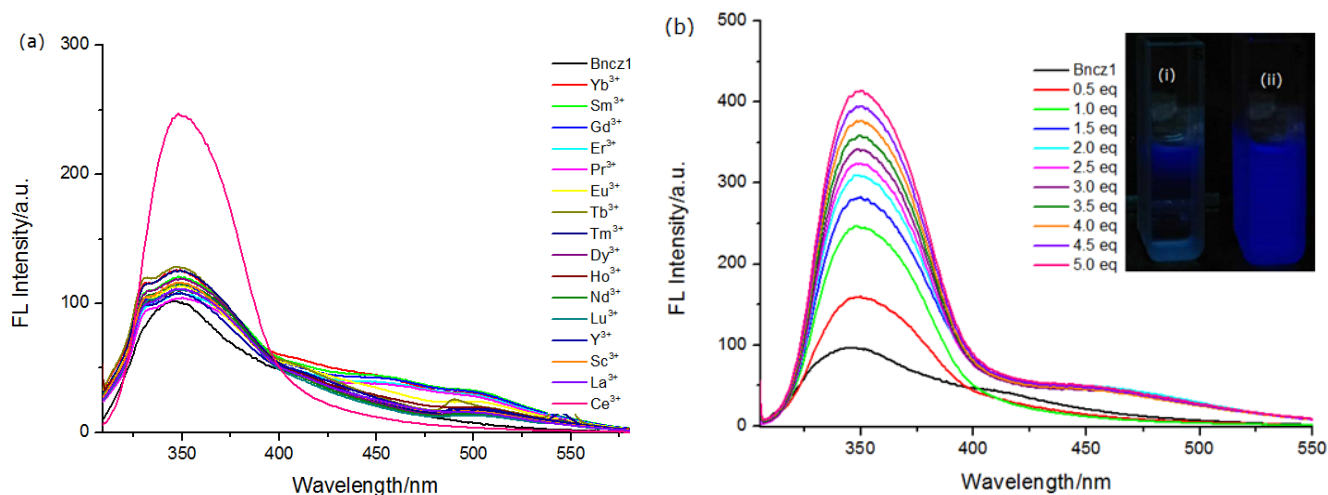


**Figure 2.** (a) Fluorescence emission spectra of **Bncz 1** observed upon addition of 1.0 equiv. of various metal ions in EtOH ( $10 \mu\text{M}$ ),  $\lambda_{\text{ex}} = 300 \text{ nm}$ ; (b) Fluorescence emission spectra of **Bncz 1** with 1.0-5.0 equivalent of  $\text{Ce}(\text{NO}_3)_3$  in ethanol ( $10 \mu\text{M}$ ),  $\lambda_{\text{ex}} = 300 \text{ nm}$ . Inset: Images showing the emission colors of (i) **Bncz 1**, (ii) **Bncz 1** with  $\text{Ce}^{3+}$  (1:1) under UV light illumination.

The **Bncz 1** fluorescence response was examined using the well known Benesi–Hildebrand (BH) equation.<sup>20,21</sup> As shown in **Figure 3**, under the optimum conditions, there is a good linear relationship between the relative UV–vis absorption and the concentration of  $\text{Ce}^{3+}$  with a correlation coefficient ( $R^2$ ) of 0.9912. A moderate association constant of  $K = 2.419 \times 10^5 \text{ L}\cdot\text{mol}^{-1}$  has been determined by fluorescence titration for  $\text{Ce}^{3+}$ –**Bncz 1** (**Figure 3**). The linear changes in UV–vis absorption and fluorescence intensity in response to different concentrations of  $\text{Ce}^{3+}$  gives a low detection limit of  $5.23 \times 10^{-6} \text{ M}$  or  $7.27 \times 10^{-6} \text{ M}$ , respectively (**Figure 4a** and **4b**). The corresponding Job's plot analysis indicated 1:1 binding for metal complex formation (**Figure 5**).

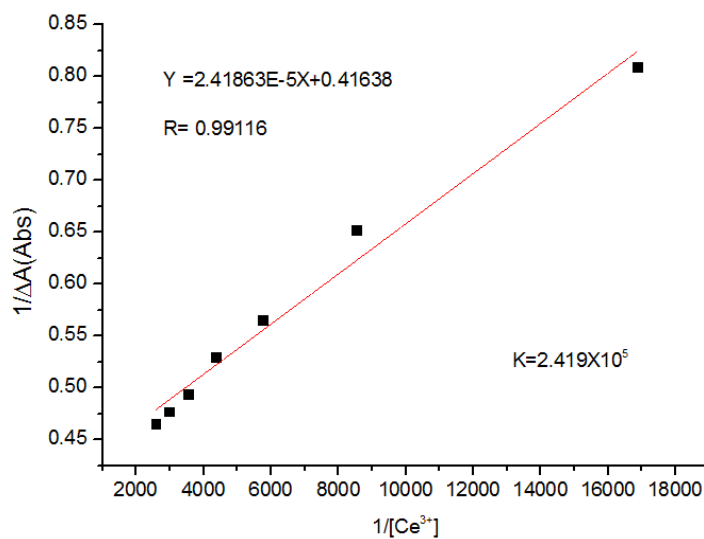


Figure 3. Benesi-Hildebrand plot of Ce<sup>3+</sup>-Bncz 1 in EtOH

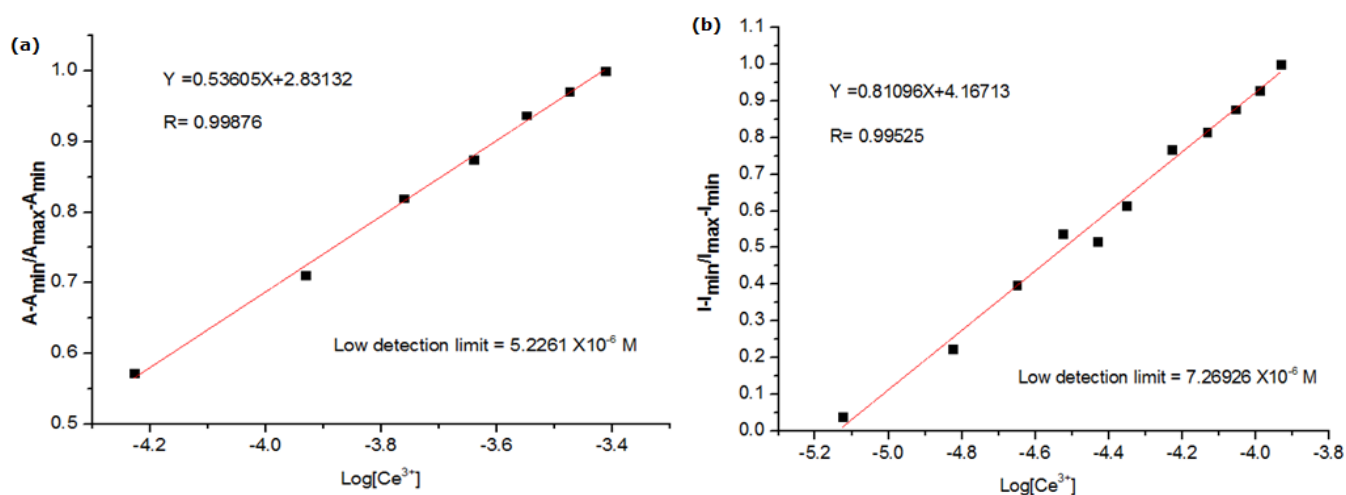
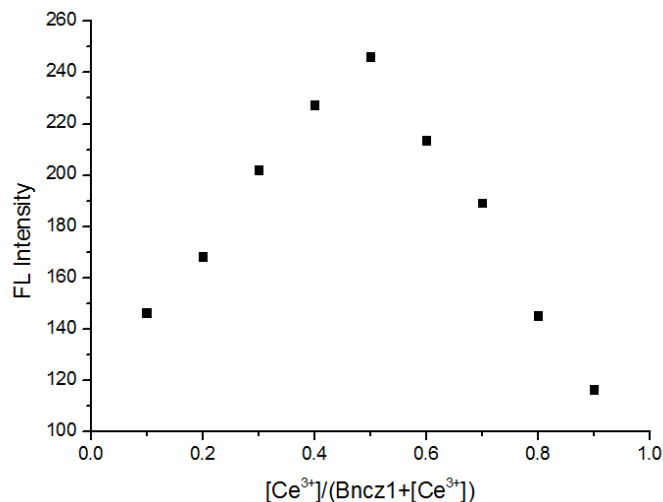
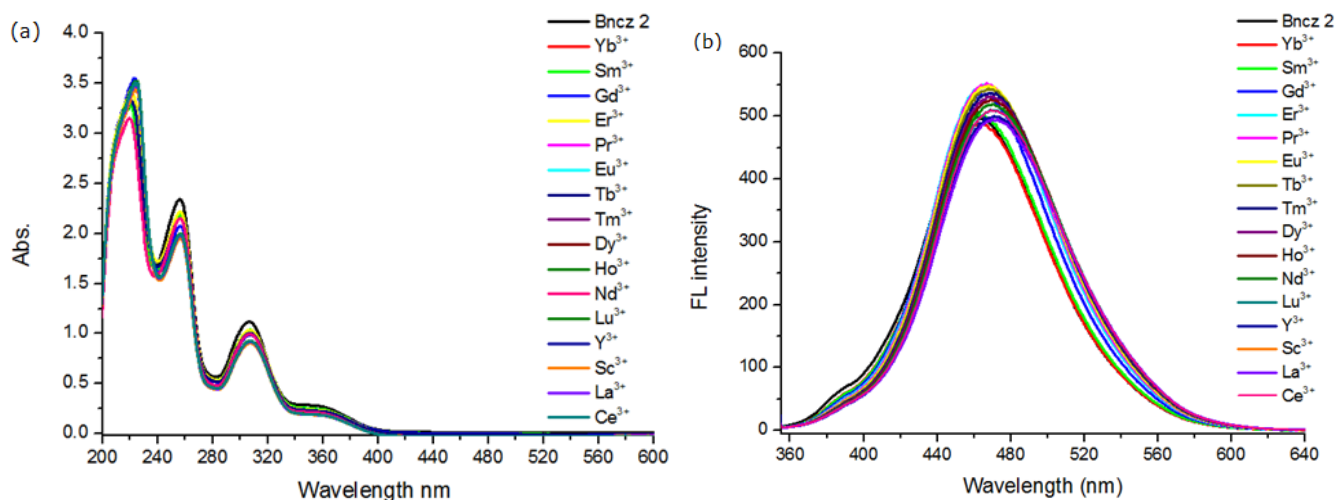


Figure 4. (a) Benesi-Hildebrand plot obtained from the UV- vis absorption (absorption calculated from 224 nm) for Ce<sup>3+</sup>-Bncz 1; (b) Benesi-Hildebrand plot obtained from the fluorescence emission spectra ( $\lambda_{em} = 346$  nm) for Ce<sup>3+</sup>-Bncz 1 in EtOH.



**Figure 5.** Job's plot of probe **Bncz 1** and  $\text{Ce}^{3+}$ ,  $\lambda_{\text{ex}}=300$  nm

In order to demonstrate the influencing factors of selectivity and sensitivity, we synthesized a **Bncz 2** (**Scheme 1, down**). The UV–vis absorption and fluorescence spectra of **Bncz 2** showed the absorption of 220, 256, 306, 356 nm, respectively. In contrast to **Bncz 1**, the obtained spectrum is quite similar to that of **Bncz 2** (**Figure 6a** and **6b**). By the same taken, 1-position of the carbazole, ethyl 1-methyl-9*H*-carbazole-2-carboxylate was hardly applicable for the recognition of Ce(III) ion under the standard condition.



**Figure 6.** (a) UV–vis absorption spectra of **Bncz 2** observed on addition of 1.0 equiv. of various metal ions in EtOH ( $10 \mu\text{M}$ ); (b) Fluorescence emission spectra of **Bncz 2** observed on addition of 1.0 equiv. of various rare earth metal ions in EtOH ( $10 \mu\text{M}$ ),  $\lambda_{\text{ex}}=300$  nm.

### Effect of pH on Fluorescence Intensity

Generally, pH is one of the major variables that affect the fluorescence of organic compound.<sup>22,23</sup> Carbazole derivatives are sensitive to their surrounding chemicals such as acids, bases.<sup>6,24,25</sup> To further evaluate the practicality of probe **Bncz 1** for  $\text{Ce}^{3+}$  detection, influence of pH on fluorescence intensity changes of probe **Bncz 1** (at 346 nm) with and without  $\text{Ce}^{3+}$  was also investigated (**Figure 7**). As shown in **Figure 7**, the fluorescence intensity was studied against pH in the range between 2.0 and 12.0 in order to obtain the optimum conditions for determination of  $\text{Ce}^{3+}$  ion. **Bncz 1** fluorescence intensity could be directly correlated with pH values. The  $\text{Ce}^{3+}$  induced fluorescence enhancement of **Bncz 1** was observed within pH range from 4.0 to 7.0, suggesting that **Bncz 1** could be used for  $\text{Ce}^{3+}$  detection at near neutral or weak acidic medium. Therefore, the optimum net fluorescence intensity was obtained in the pH range of 4.0 and 7.0, and weak acid and neutral solution was used for the determination of  $\text{Ce}^{3+}$  ion study.

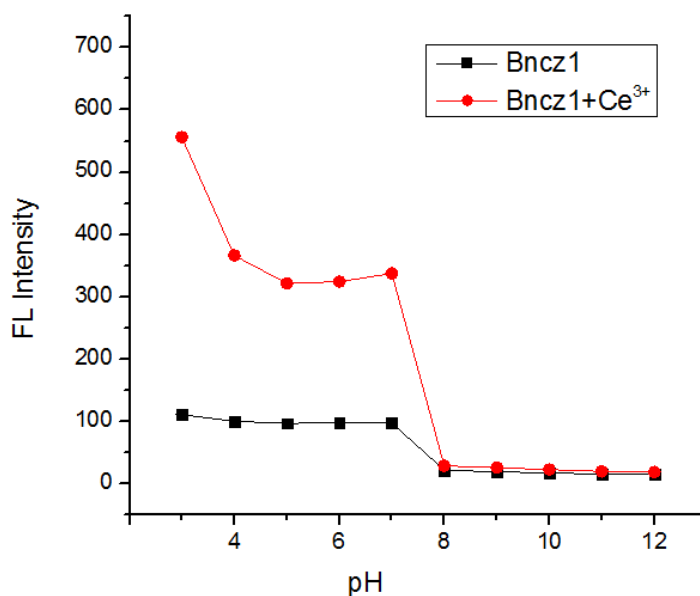
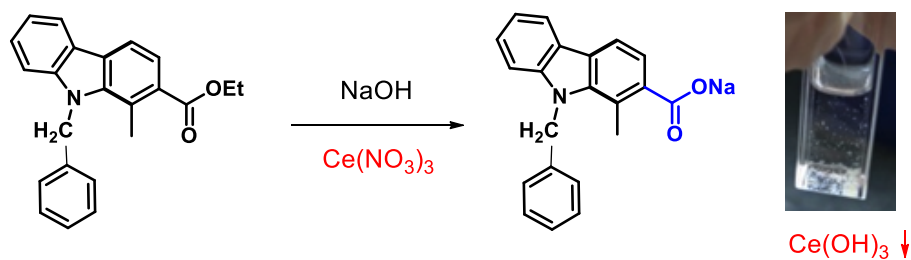


**Figure 7.** Fluorescence intensity (at 346 nm) changes of **Bncz 1** (10  $\mu\text{M}$ ) with and without  $\text{Ce}^{3+}$  ions in EtOH solution (10  $\mu\text{M}$ ) at different pH conditions at 25 °C,  $\lambda_{\text{ex}} = 300 \text{ nm}$

In the beginning, as shown in **Figure 7**, we supposed that **Bncz 1** showed effective sensing response may be due to the existence of  $\text{Ce}^{3+}$  cation could be stabilized in acidic medium, and the concentration of  $\text{Ce}^{3+}$  decreases because of the formation of  $\text{Ce}(\text{OH})_3$  in alkaline medium.<sup>26</sup> This leads to a decrease in the fluorescence intensity with an increase in pH. At higher pH (pH > 8.0) the fluorescence intensity decreases due to the existence of  $\text{OH}^-$  groups on the surface of **Bncz 1** which hinders the interaction between  $\text{Ce}^{3+}$  and **Bncz 1**. At the same time, a saponification reaction of **Bncz 1** could take place and form some insoluble hydroxy complexes of  $\text{Ce}^{3+}$  in the alkaline medium, thus losing its fluorescence ability, as shown in the following chemical formula (**Scheme 2**).



**Scheme 2.** A saponification reaction of **Bncz 1** and sodium hydroxide and the formation of Ce(OH)<sub>3</sub> in alkaline medium

However, we detected the FT-IR spectra of **Bncz 1** without Ce(NO<sub>3</sub>)<sub>3</sub> in different pH. The FT-IR spectra of the **Bncz 1** (pH=7, top) and **Bncz 1** (pH=2 or 10) compared to each other (see **Figure 8**). The ester carbonyl of 9-benzyl-9*H*-carbazole stretching band can be clearly seen at 1715 cm<sup>-1</sup> of **Bncz 1** spectrum (pH=7). Absence of this peak in the FT-IR spectrum of **Bncz 1** in pH=2 or 10 proves the ester carbonyl of 9-benzyl-9*H*-carbazole derivative is sensitive to the strong acids or bases.<sup>27</sup> Thus, the effect of pH on the fluorescence intensity of Ce<sup>3+</sup>-**Bncz 1** system was studied to obtain the optimum pH to develop a sensitive fluorescence sensor for Ce<sup>3+</sup> ion.

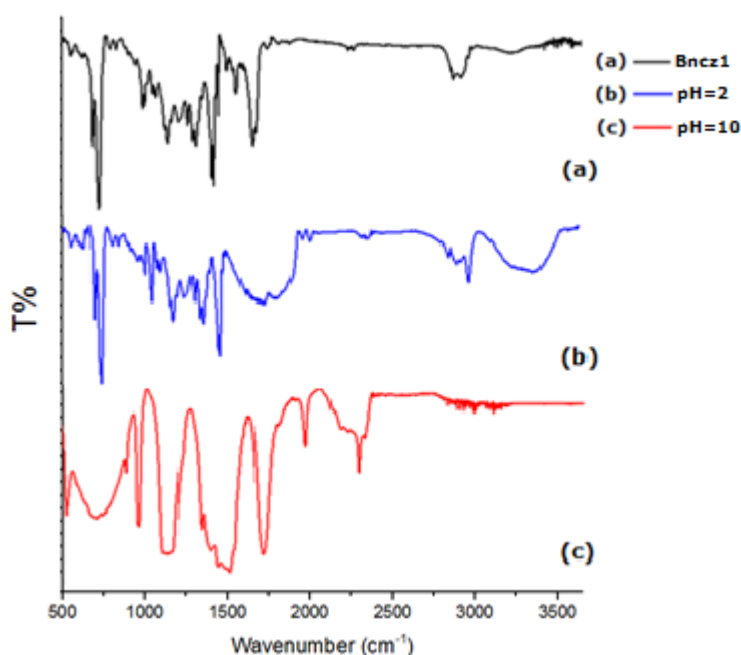
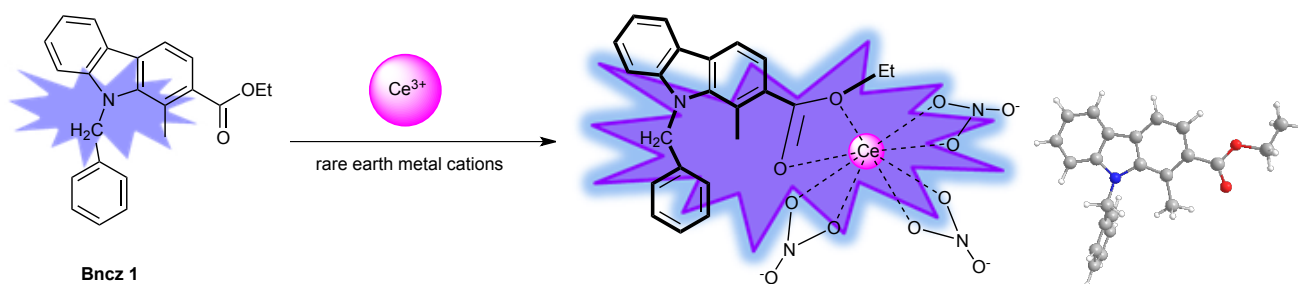


**Figure 8.** FT-IR spectra of **Bncz 1** without Ce(NO<sub>3</sub>)<sub>3</sub> in different pH

These results suggested that the ester carbonyl of 9-benzyl-9*H*-carbazole derivative in a chemosensor play an important role in the selectivity. It is hypothesized that the strong binding of **Bncz 1** with the Ce<sup>3+</sup> cations could be on account of the strong electron-donating properties of the ester carbonyl, which

significantly increase the electron density on the carbazole cyclic  $\pi$ -conjugation, hence facilitating the binding of **Bncz 1** with the  $\text{Ce}^{3+}$  cation.

Therefore, we surmise that the recognition of  $\text{Ce}^{3+}$  cation is dependent on their size and outer electronic structure. Ce(III) have larger ionic radius than the other rare earth metal cations and an unoccupied 5d orbital, which apparently leads to geometric and electronic matching with the ligand **Bncz 1** in Scheme 3.



**Scheme 3.** The proposed binding modes of **Bncz 1** with  $\text{Ce}^{3+}$  and an optimized conformation of **Bncz 1**

In conclusion, we have developed a novel ratiometric fluorescent probe based on 9-benzyl-9*H*-carbazole derivative, which has been applied for the recognition of rare earth metal cations at near neutral or weak acidic medium. Ethyl 9-benzyl-1-methyl-9*H*-carbazole-2-carboxylate chemosensor has been applied for the unique recognition of  $\text{Ce}^{3+}$ . A moderate association constant of  $K = 2.419 \times 10^5 \text{ L mol}^{-1}$  has been determined by fluorescence titration, and the corresponding Job's plot analysis indicated 1:1 binding for metal complex formation. The linear increase in fluorescence intensity in response to different concentrations of  $\text{Ce}^{3+}$  gives a low limit of detection of  $7.269 \times 10^{-6} \text{ M}$ . Therefore, this 9-benzyl-9*H*-carbazole derivative probe has a great potential for the detection of rare earth metal cations. We plan to keep exploring the scope and synthetic application of carbazole derivatives in solution by photophysical properties in our laboratory.

## EXPERIMENTAL

### Materials and apparatus

3-(2,2-Diethoxyethyl)-1,3-dicarbonyl compounds and [BPy]HSO<sub>4</sub> were prepared according to a known method.<sup>28</sup> The various rare earth metal nitrates were obtained commercially and used without further purification. <sup>1</sup>H and <sup>13</sup>C NMR spectra were recorded on a Bruker AV-500. Chemical shifts were reported in ppm relative to TMS in CDCl<sub>3</sub>. IR spectra was recorded on a Nicolet Nexus 670 FT spectrometer in KBr with absorptions in cm<sup>-1</sup>. UV-vis absorption spectra were recorded with UV-2700 (Shimadzu) at room temperature. Fluorescence emission spectra were recorded on a RF-5301(PC)-S-93 (Shimadzu) fluorescence spectrophotometer at 25 °C. The GAUSSIAN 03 program was used to optimise the structure and obtain in the present work. The hartree-fock method was used for both geometry optimization. The 6-311G(3df,3dp) basis set for C, N, O and H were used.

### Synthesis of 9-benzyl-9H-carbazole derivatives

Ethyl 9-benzyl-1-methyl-9H-carbazole-2-carboxylate (**Bncz 1**) and 1-(9-benzyl-1-methyl-9H-carbazol-2-yl)ethanone (**Bncz 2**) were prepared and purified according to the methods developed in our laboratory.<sup>29</sup> In a 10 mL of V type tube equipped with a triangle stirring bar, MeCN (1.0 mL), 1-benzylindole (0.25 mmol), 3-(2,2-diethoxyethyl)-1,3-dicarbonyl compounds (0.38 mmol) and [BPy]HSO<sub>4</sub> (0.025 mmol) were added. The mixture was stirred at room temperature (15 °C) for 24 h. After that, the volatile component was removed under reduced pressure. Then, the product was extracted with a mixture composed of EtOAc and heptane (v/v = 2/1, 1 mL × 3). The organic phase was combined and concentrated under reduced pressure. The product **Bncz 1** and **Bncz 2** were isolated by preparative TLC by using a mixture of EtOAc and petroleum ether (v/v = 1/5) as eluting solvent.

### Spectroscopic Data of **Bncz 1** and **Bncz 2**

Ethyl 9-benzyl-1-methyl-9H-carbazole-2-carboxylate (**Bncz 1**): 55.8 mg, 65%; colorless oil; <sup>1</sup>H NMR (500 MHz, CDCl<sub>3</sub>, 25 °C, TMS):  $\delta$  = 1.45 (t, *J* = 7.5 Hz, 3H), 3.05 (s, 3H), 4.43 (q, *J* = 7.0 Hz, 2H), 5.73 (s, 2H), 7.03–7.05 (d, 2H), 7.23–7.27 (m, 5H), 7.40–7.45 (m, 2H), 7.98 (d, 1H), 8.10 (d, 1H) ppm; <sup>13</sup>C NMR (125 MHz, CDCl<sub>3</sub>, 25 °C):  $\delta$  = 14.9, 15.6, 48.5, 61.8, 100.8, 108.9, 116.8, 119.2, 119.3, 119.7, 120.0, 121.8, 124.9, 125.3, 126.4, 126.7, 128.3, 137.8, 137.8, 139.7, 142.5, 169.9 ppm; IR:  $\nu$  = 2977, 1715, 1559, 1461, 1413, 1375, 1201, 1040, 916, 813, 745 cm<sup>-1</sup>; Anal. Calcd for C<sub>23</sub>H<sub>21</sub>NO<sub>2</sub>: C, 80.44; H, 6.16. Found: C, 80.33; H, 6.10.

1-(9-Benzyl-1-methyl-9H-carbazol-2-yl)ethanone (**Bncz 2**): 65.0 mg, 83%; yellow oil; <sup>1</sup>H NMR (500 MHz, CDCl<sub>3</sub>, 25 °C, TMS):  $\delta$  = 2.67 (s, 3H), 2.73 (s, 3H), 5.78 (s, 2H), 7.08 (d, 2H), 7.26–7.32 (m, 5H), 7.45–7.49 (m, 2H), 8.02 (d, 1H), 8.14 (d, 1H) ppm; <sup>13</sup>C NMR (125 MHz, CDCl<sub>3</sub>, 25 °C):  $\delta$  = 14.1, 30.9, 49.1, 101.4, 109.5, 117.4, 119.8, 119.9, 120.3, 120.5, 122.4, 125.5, 125.9, 127.0, 127.3, 128.9, 138.3, 138.4, 140.3, 143.1, 203.7 ppm; IR:  $\nu$  = 2965, 2923, 2852, 1656, 1498, 1452, 1416, 1127, 1031, 801, 741 cm<sup>-1</sup>; Anal. Calcd for C<sub>22</sub>H<sub>19</sub>NO: C, 84.31; H, 6.11. Found: C, 84.17; H, 6.03.

### Spectroscopic measurements

#### UV–vis absorption and fluorescence spectra measurements

The stock solution of **Bncz 1** or **Bncz 2** (1.0 mM) was prepared in MeCN, which was further diluted with EtOH to 10  $\mu$ M for UV–vis absorption and fluorescence spectra measurements respectively. The selectivity experiments were conducted by addition the same doses of metal ions into **Bncz 1** or **Bncz 2** assay solution at 25 °C. Fluorescence spectroscopic experiments were carried out in 10-mm quartz cuvettes with excitation at  $\lambda_{\text{ex}}$  = 300 nm at 25 °C, respectively. For titration experiments, different doses of Ce<sup>3+</sup> were added into the **Bncz 1/Bncz 2** solution and measure the UV–vis absorption/fluorescence spectrum changes at 25 °C. The band-slits of both excitation and emission were set at 3 or 5 nm and the scan speed was 1200 nm·min<sup>-1</sup>.

Stock solutions were prepared with 5 mM concentration of various rare earth metal nitrate salts in double-distilled water. A series of EtOH solutions of **Bncz 1** or **Bncz 2** was added 1.0 equiv. of the following metal nitrate salts, Yb(NO<sub>3</sub>)<sub>3</sub>·5H<sub>2</sub>O, Sm(NO<sub>3</sub>)<sub>3</sub>·6H<sub>2</sub>O, Gd(NO<sub>3</sub>)<sub>3</sub>·6H<sub>2</sub>O, Er(NO<sub>3</sub>)<sub>3</sub>·6H<sub>2</sub>O, Pr(NO<sub>3</sub>)<sub>3</sub>·6H<sub>2</sub>O, Eu(NO<sub>3</sub>)<sub>3</sub>·6H<sub>2</sub>O, Tb(NO<sub>3</sub>)<sub>3</sub>·6H<sub>2</sub>O, Tm(NO<sub>3</sub>)<sub>3</sub>·6H<sub>2</sub>O, Dy(NO<sub>3</sub>)<sub>3</sub>·6H<sub>2</sub>O, Ho(NO<sub>3</sub>)<sub>3</sub>·5H<sub>2</sub>O, Nd(NO<sub>3</sub>)<sub>3</sub>·6H<sub>2</sub>O, Lu(NO<sub>3</sub>)<sub>3</sub>·6H<sub>2</sub>O, Y(NO<sub>3</sub>)<sub>3</sub>·6H<sub>2</sub>O, Sc(NO<sub>3</sub>)<sub>3</sub>·6H<sub>2</sub>O, La(NO<sub>3</sub>)<sub>3</sub>·6H<sub>2</sub>O, Ce(NO<sub>3</sub>)<sub>3</sub>·6H<sub>2</sub>O, respectively.

### pH effect evaluation

The EtOH solution of the probe (10 μM) was adjusted to different pH values with 10% HCl or 10% aqueous NaOH solutions and pH-indicator paper was used to measure pH values of EtOH solution. The solutions were subjected to fluorescence detection after the solutions were allowed to stand for 24 h. Then 1.0 equiv. of Ce<sup>3+</sup> was added into the above prepared probe solutions with different pH values, and the fluorescence of the solution was checked.

### ACKNOWLEDGEMENTS

The authors are thankful to the Research Funds of CaoYuanYingCai Program of Inner Mongolia (841060) for the financial support.

### REFERENCES

1. (a) J. Qiu, Q. Jiao, D. Zhou, and Z. Yang, *J. Rare Earth*, 2016, **34**, 341; (b) M. Wang, M. Li, A. Yu, J. Wu, and C. Mao, *ACS Appl. Mater. Interfaces*, 2015, **7**, 28110; (c) G. Han, S. Zhang, Z. Xing, and X. Zhang, *Angew. Chem. Int. Ed.*, 2013, **52**, 1466.
2. T. A. Ali, G. G. Mohamed, EMS Azzam, and A. A. Abd-elaal, *Sensor Actuat. B-Chem.*, 2014, **191**, 192.
3. A. Afkhami, T. Madrakian, A. Shirzadmehr, M. Tabatabaee, and H. Bagheri, *Sensor Actuat. B-Chem.*, 2012, **174**, 237.
4. (a) V. Matsouka, M. Konsolakis, I. V. Yentekakis, A. Papavasiliou, and A. Tsetsekou, *Top. Catal.*, 2009, **52**, 1873; (b) R. Yuvaraja, K. Nanthakumar, and G. Dhasahinamoorthi, *Aust. J. Basic Appl. Sci.*, 2015, **9**, 471.
5. H. J. Knölker and K. R. Reddy, *Chem. Rev.*, 2002, **102**, 4303.
6. A. W. Schmidt, K. R. Reddy, and H. J. Knölker, *Chem. Rev.*, 2012, **112**, 3193.
7. C. Ito, M. Itoigawa, A. Sato, C. M. Hasan, M. A. Rashid, H. Tokuda, T. Mukainaka, H. Nishino, and H. Furukawa, *J. Nat. Prod.*, 2004, **67**, 1488.
8. F. F. Zhang, L. L. Gan, and C. H. Zhou, *Bioorg. Med. Chem. Lett.*, 2010, **20**, 1881.
9. F. Dumur, *Org. Electron.*, 2015, **25**, 345.
10. J. P. Lellouche, R. R. Koner, and S. Ghosh, *Rev. Chem. Eng.*, 2013, **29**, 413.
11. J. Li and A. C. Grimsdale, *Chem. Soc. Rev.*, 2010, **39**, 2399.
12. J. V. Grazulevicius, P. Strohriegel, J. Pielichowski, and K. Pielichowski, *Prog. Polym. Sci.*, 2003, **28**,

1297.

13. J. Dong, Y. Liu, J. Hu, H. Baigude, and H. Zhang, *Sensor Actuat. B-Chem.*, 2018, **255**, 952.
14. Y. Bao, B. Liu, H. Wang, F. Du, and R. Bai, *Anal. Methods*, 2011, **3**, 1274.
15. S. Sinha, S. Kumar, R. R. Koner, J. Mathew, C. K. Nandi, and S. Ghosh, *RSC Adv.*, 2013, **3**, 6271.
16. Y. Huang, Q. Geng, X. Jin, H. Cong, F. Qiu, L. Xu, Z. Tao, and G. Wei, *Sensor Actuat. B-Chem.*, 2017, **243**, 1102.
17. (a) G. Tircso, Z. Kovacs, and A. D. Sherry, *Inorg. Chem.*, 2006, **45**, 9269; (b) F. Yan, K. Fan, J. Xu, J. Wang, C. Ma, and T. Ma, *Spectrochim. Acta A*, 2019, **213**, 254.
18. W. Xia, R. H. Schmehl, and C. Li, *Tetrahedron*, 2000, **56**, 7045.
19. S. J. Barrow, S. Kasera, M. J. Rowland, J. Barrio, and O. A. Scherman, *Chem. Rev.*, 2015, **115**, 12320.
20. M. Shortreed, R. Kopelman, M. Kuhn, and B. Hoyland, *Anal. Chem.*, 1996, **68**, 1414.
21. X. Yang, B. Yang, J. Ge, Y. Xu, Q. Xu, J. Liang, and J. Lu, *Org. Lett.*, 2011, **13**, 2710.
22. (a) Y. Jiang, L. Sun, G. Ren, X. Niu, W. Hu, and Z. Hu, *ChemistryOpen*, 2015, **4**, 378; (b) L. Tang, S. Ding, X. Zhang, K. Zhong, S. Hou, and Y. Bian, *J. Photochem. Photobiol. A: Chem.*, 2017, **340**, 15.
23. M. K. Rofouei, N. Tajarrood, M. Masteri-Farahani, and R. Zadmard, *J. Fluoresc.*, 2015, **25**, 1855.
24. X. Jiao, Z. Xiao, P. Hui, C. Liu, Q. Wang, X. Qiu, S. He, X. Zeng, and L. Zhao, *Dyes Pigm.*, 2019, **160**, 633.
25. S. J. Malthus, S. A. Cameron, and S. Brooker, *Inorg. Chem.*, 2018, **57**, 2480.
26. (a) J. Aldana, N. Lavelle, Y. Wang, and X. Peng, *J. Am. Chem. Soc.*, 2005, **127**, 2496; (b) M. Gao, S. Kirstein, H. Möhwald, A. L. Rogach, A. Kornowski, A. Eychmüller, and H. Weller, *J. Phys. Chem. B*, 1998, **102**, 8360.
27. C. David, S. Guzman, R. A. Carmen, T. Alberto, and M. Pedro, *Org. Biomol. Chem.*, 2012, **10**, 1896.
28. (a) Y. Du, F. Tian, and W. Zhao, *Synth. Commun.*, 2006, **36**, 1661; (b) V. M. Ismailov, N. N. Yusubov, N. D. Sadykhova, R. A. Gasymov, G. G. Ibragimova, and I. A. Mamedov, *Russ. J. Org. Chem.*, 2016, **52**, 1390.
29. Y. Du, W. Xue, R. Gao, Y. Gu, and L. Han, *Tetrahedron Lett.*, 2018, **59**, 4221.